

# Preparation and catalytic application of MCM-41 modified with a ferrocene carboxyphosphine and a ruthenium complex<sup>☆</sup>

Petr Štěpnička<sup>a,\*</sup>, Jan Demel<sup>a,b</sup>, Jiří Čejka<sup>b</sup>

<sup>a</sup> Department of Inorganic Chemistry, Faculty of Science, Charles University, Hlavova 2030, CZ-128 40 Prague 2, Czech Republic

<sup>b</sup> J. Heyrovský Institute of Physical Chemistry, Academy of Sciences of the Czech Republic, Dolejškova 3, CZ-182 23 Prague 8, Czech Republic

Received 16 March 2004; received in revised form 27 July 2004; accepted 30 July 2004

Dedicated to Professor Jozef J. Ziolkowski on the occasion of his 70th birthday.

## Abstract

Reaction of 1'-(diphenylphosphino)ferrocenecarboxylic acid (Hdpf) with mesoporous molecular sieve MCM-41 gives immobilized carboxyphosphine (**3**), which was further reacted with  $[\{\text{Ru}(\eta^6\text{-}p\text{-cymene})\text{Cl}(\mu\text{-Cl})\}_2]$  (**1**) to afford Ru/carboxyphosphine-modified molecular sieve **4**. A simple reaction between MCM-41 and **1** afforded Ru-only modified molecular sieve **5**.

Materials **4** and **5** were tested as catalysts for the reaction of propargyl alcohol with benzoic acid to give 2-oxopropyl benzoate (**6**). The reactions catalyzed with immobilized catalysts are slower and give lower yields of the ester as compared to the homogeneous precatalyst  $[\text{Ru}(\eta^6\text{-}p\text{-cymene})(\text{Hdpf-}\kappa\text{P})\text{Cl}_2]$  (**2**), which was prepared from Hdpf and the dimer **1**. Formation of ester **6** catalyzed with **4** and **5** competes with a parallel, propargyl alcohol consuming process, which occurs also with MCM-41 itself in the absence of benzoic acid and ruthenium compounds. The solid-state structure of  $2\cdot\text{CH}_2\text{Cl}_2$  has been determined by single-crystal X-ray diffraction.

© 2004 Elsevier B.V. All rights reserved.

**Keywords:** Ferrocene carboxyphosphine; MCM-41; Ruthenium; Immobilization; 2-Oxopropyl benzoate; X-ray crystallography

## 1. Introduction

Catalytic systems involving ferrocene ligands proved often superior to analogous systems with classical organic ligands. As a result, ferrocene ligands have found widespread practical applications even at the industry scale [1]. Since immobilized catalytic systems are usually more chemically robust, easier separable and recyclable (etc.) than their homogeneous counterparts and thus attractive from economical and ecological viewpoints, attempts have been made to attach ferrocene ligands to solid supports. Anchoring of ferrocene compounds has been achieved by reacting a ferrocene ligand or its complex modified with a suitable, mostly amidosilox-

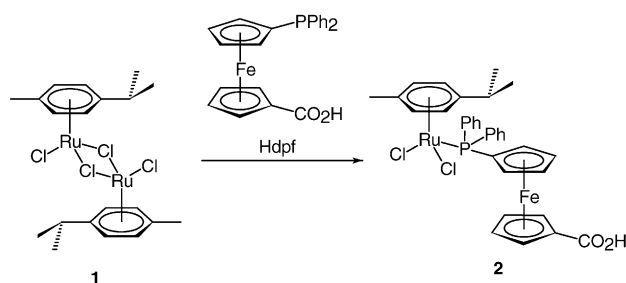
ane, linker with a solid matrix, typically silica [2]. Another, apparently more suitable solid supports worth testing for immobilization of homogeneous organometallic catalysts are mesoporous molecular sieves.

A new era in the investigation of mesoporous molecular sieves started with the successful synthesis of these materials at Mobil Research and Development Corporation in early 1990s [3]. Mesoporous molecular sieves are prepared by using template strategy with supramolecular surfactant assemblies (e.g., long-chain alkyl amines, carboxylic acids or triblock copolymers) to form inorganic building blocks with the required geometry [4,5]. They exhibit uniform pores of hexagonal or cubic ordering with pore dimensions ranging from 2.0 to about 30 nm, surface areas often larger than 1000 m<sup>2</sup>/g, amorphous walls and long-range ordering [6]. The large surface areas and narrow pore size distribution as compared to conventional materials [7] make the utility of molecular sieves as a support for organometallic

<sup>☆</sup> Presented at the 14th International Conference on Homogeneous Catalysis in Munich, Germany. For a reference, see Books of Abstracts, p. 206.

\* Corresponding author.

E-mail address: [stepnic@natur.cuni.cz](mailto:stepnic@natur.cuni.cz) (P. Štěpnička).

Scheme 1. Preparation of the molecular catalyst **2**.

catalysis particularly attractive. This has been recently evidenced by a number of examples including immobilization of an osmium-tertiary diolate complex for *cis*-dihydroxylation of double bonds [8], anchoring [ $\{\text{Rh}(\eta^2\text{-}\eta^2\text{-cycloocta-1,5-diene})(\mu\text{-OCH}_3)\}_2$ ] complex on MCM-41 and its conversion to an immobilized hydride complex, which was highly active in polymerization of phenylethyne and its ring-substituted derivatives [9], and also by immobilization of chiral ferrocene catalysts [10].

Considering the abovementioned properties and applications of mesoporous molecular sieves, we decided to study a system based on carboxy-functionalized ferrocenyldiphosphine, 1,1'-(diphenylphosphino)ferrocenecarboxylic acid (Hdpf) [11], and MCM-41, where the conformationally flexible 1,1'-disubstituted ferrocene unit may act as a spacer between the anchoring (carboxyl) and catalytic (phosphine) sites. In this contribution, we describe the preparation and characterization of MCM-41 sieves modified with [ $\{\text{Ru}(\eta^6\text{-}p\text{-cymene})\text{Cl}(\mu\text{-Cl})\}_2$ ] and Hdpf. We also report on the activity of the Ru-modified materials as catalysts in ruthenium-catalyzed reaction between benzoic acid and propargylalcohol to synthetically valuable 2-oxopropyl benzoate [12]—in a comparison with a molecular precatalyst [ $\text{Ru}(\eta^6\text{-}p\text{-cymene})(\text{Hdpf-}\kappa\text{P})\text{Cl}_2$ ].

## 2. Results and discussion

### 2.1. Preparation and characterization of the molecular catalysts

Complex [ $\text{Ru}(\eta^6\text{-}p\text{-cymene})(\text{Hdpf-}\kappa\text{P})\text{Cl}_2$ ] (**2**) was synthesized in nearly quantitative yield by cleavage of the chloro bridges in dimeric ruthenium(II) complex [ $\{\text{Ru}(\eta^6\text{-}p\text{-cymene})\text{Cl}(\mu\text{-Cl})\}_2$ ] (**1**) with stoichiometric amount of Hdpf (Scheme 1). The identity and purity of the complex were confirmed by NMR, IR, mass spectrometry, elementary analysis and by single-crystal X-ray diffraction.  $^1\text{H}$  and  $^{13}\text{C}$  NMR spectra of **2** are in full accordance with the proposed three-legged piano stool structure [ $(\eta^6\text{-arene})\text{RuCl}_2(\text{phosphine-}\kappa\text{P})$ ]. This is mainly manifested by a significantly up-field shifted carbon and hydrogen resonances due to the arene CH groups ( $\delta_{\text{C}}$  85–91,  $\delta_{\text{H}}$  5.10–5.20) and their couplings with Ru-bonded phosphorus atom (arene CH resonances in  $^{13}\text{C}$  NMR

spectra;  $^2J_{\text{PC}} = 4.3$  and  $5.9$  Hz). The  $^{31}\text{P}$  NMR coordination shift of **2** ( $\Delta_{\text{P}} = 36.9$ ,  $\Delta_{\text{P}} = \delta_{\text{P,complex}} - \delta_{\text{P,free ligand}}$ ) is very similar to its analogue with  $\eta^6$ -hexamethylbenzene ligand [13], whereas the  $\delta_{\text{P}}$  value itself is slightly down-field from the reference compound, due to a lowered electron density at the metal centre and, hence, at the phosphorus atom, resulting from the presence of a less electron donating arene ligand. The matrix mass spectra of **2** exhibit fragment ions corresponding to the loss of one or two chloride ligands ( $[\text{M}-n\text{Cl}]^+$ ,  $n = 1, 2$ ), fragments resulting from an elimination of the carboxycyclopentadienyl ring and iron atom,  $[\text{M}-\text{C}_6\text{H}_5\text{O}_2\text{Fe}]^+$ , and ions due to phosphine cation ( $\text{Hdpf}^+$ ).

### 2.2. The solid-state structure of **2**

Recrystallization of **2** from dichloromethane-hexane afforded the solvate **2**· $\text{CH}_2\text{Cl}_2$ , which was characterized by single-crystal X-ray diffraction analysis. The compound crystallizes with two crystallographically independent but structurally nearly identical molecules within the unit cell (A and B). A view of the molecular structure of molecule A is shown in Fig. 1 and the selected geometric parameters for both crystallographically independent molecules are listed in Table 1. The overall molecular geometry is rather unexceptional when compared to the related arene–ruthenium complexes with ferrocene phosphines such as: [ $\{\mu\text{-}1\kappa\text{P}:2\kappa\text{P}'\text{-Fe}(\eta^5\text{-C}_5\text{H}_4\text{CH}_2\text{PPh}_2)_2\}\{\text{RuCl}_2(\eta^6\text{-C}_6\text{H}_2\text{Me}_4\text{-}1,2,3,4)\}_2$ ] [14], and [ $\text{Ru}\{\text{C}(\text{CH}_2\text{Fc})\text{OMe}\}(\eta^6\text{-C}_6\text{Me}_6)\text{Cl}(\text{Hdpf-}\kappa\text{P})\}\cdot\text{CH}_2\text{Cl}_2$  (Fc = ferrocenyl) [13].

The molecules of **2** associate into dimers involving both independent molecules via double hydrogen bridges between their peripheral carboxy groups,  $\text{A}\cdots\text{B}$  (Table 2). This arrangement is frequently encountered in complexes where Hdpf coordinates as a simple phosphine [15] as well as in Hdpf itself [11]. The dimers are linked further by weak hydrogen bonds to solvating dichloromethane (Table 2). Hydrogen bonding is apparently the major force towards intermolecular association in **2**· $\text{CH}_2\text{Cl}_2$  since neither significant  $\pi\cdots\pi$  stacking interactions between sterically encumbered  $\pi$ -rings nor  $\text{C-H}\cdots\pi$ -ring interactions were detected in the structure [the strongest  $\text{C-H}\cdots\pi$ -ring contacts are intramolecular:  $\text{C}(41)\text{-H}(41)\cdots\text{Ph}1$ :  $\text{C}(41)\cdots\text{Cg}43.785(4)$  Å,  $\text{C}(41)\text{-H}(41)\cdots\text{Cg}4168^\circ$ ;  $\text{C}(82)\text{-H}(82\text{C})\cdots\text{Ph}5$ :  $\text{C}(82)\cdots\text{Cg}93.562(5)$  Å,  $\text{C}(82)\text{-H}(82\text{C})\cdots\text{Cg}9158^\circ$ ; for the definition of the symbols see Table 1].

### 2.3. Preparation and characterization of supported materials

Hdpf-modified MCM-41 (**3**) was prepared by adding Hdpf solution in toluene to carefully dried molecular sieve (2 mmol/10 g), shaking the resulting suspension for 24 h and, finally, Soxhlet extraction of the solid with dichloromethane to remove unreacted Hdpf. Mass balance (the amount of recovered Hdpf) and elemental analysis showed that 84%

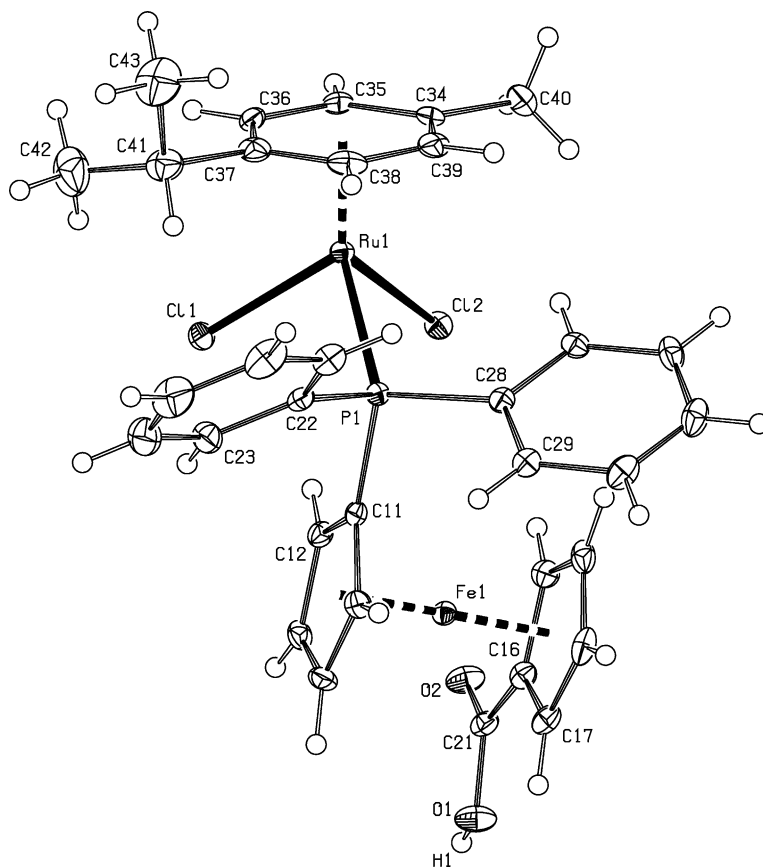


Fig. 1. A view of the molecule A in the structure of **2**-CH<sub>2</sub>Cl<sub>2</sub> showing the thermal motion ellipsoids scaled to 30% probability and atom labelling scheme.

of the carboxyphosphine remained adsorbed on the support, which corresponds to ca. 0.16 mmol of Hdpf per 1 g of the resulting material. A subsequent reaction of **3** with **1** in dichloromethane and similar workup gave Ru/phosphine modified sieve (**4**). Catalytic results (see below), prompted us to synthesize also MCM-41 modified *only* with **1**. The Ru-only modified molecular sieve (**5**) was obtained easily and with complete retention of the ruthenium complex by adding **1** dissolved in dichloromethane to solid MCM-41.

The modified sieves **3–5** were characterized by X-ray fluorescence analysis, powder X-ray diffraction, IR and solid-state NMR spectra, and textural measurements. X-ray diffraction patterns observed for the parent calcinated mesoporous MCM-41 and the modified materials (Fig. 2) exhibited five clearly discernible reflections with  $2\theta < 10^\circ$ , indicating a regular hexagonal ordering of all these mesoporous molecular sieves. The X-ray diffraction patterns of **5** (see Section 4) were identical to MCM-41 and the modified sieves **3** and **4**, thus corroborating unaffected structure of the support. The textural parameters of calcined MCM-41, **3** and **4** were determined by nitrogen adsorption isotherms recorded at  $-196^\circ\text{C}$  (Fig. 3). The adsorption isotherm of calcined MCM-41 evidenced the typically well-ordered structure of the sieve with the characteristic steep increase in the adsorbed amount at the relative pressure  $p/p_0$  ca. 0.3. Modification of the molec-

ular sieve with Hdpf (to give **3**) and further with **1** (to give **4**) decreased the surface areas and void volume of the formed composite materials. In addition, a slight decrease in the pore diameter from 3.5 nm to about 3.0 nm was observed after modification of MCM-41 molecular sieve (cf. Table 3).

IR spectra of **3** and **4** in the carbonyl stretching region (Fig. 4) showed a dominant band at  $1630\text{ cm}^{-1}$  and an unresolved, less intense band at ca.  $1700\text{ cm}^{-1}$ . The position of the bands is very similar to those in **2** ( $1702$  and  $1674\text{ cm}^{-1}$

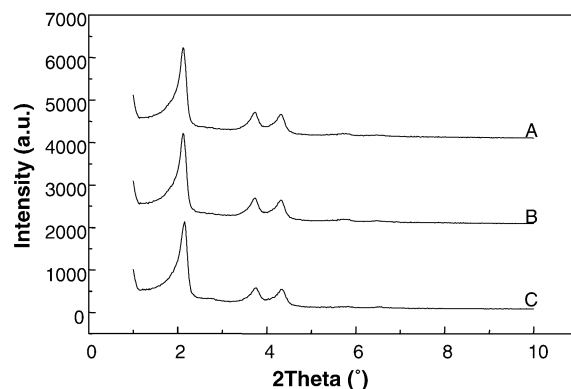


Fig. 2. Powder X-ray diffraction patterns for MCM-41 (A), **3** (B), **4** (C).

Table 1  
Selected geometric parameters for 2-CH<sub>2</sub>Cl<sub>2</sub> (in Å and °)

Molecule A		Molecule B	
Ru(1)–Cg1	1.702(1)	Ru(5)–Cg6	1.705(1)
Ru(1)–Cl(1)	2.4012(7)	Ru(5)–Cl(5)	2.4037(8)
Ru(1)–Cl(2)	2.4263(7)	Ru(5)–Cl(6)	2.4221(7)
Ru(1)–P(1)	2.3665(7)	Ru(5)–P(5)	2.3692(7)
Fe(1)–Cg2	1.658(1)	Fe(5)–Cg7	1.660(1)
Fe(1)–Cg3	1.654(1)	Fe(5)–Cg8	1.655(1)
P(1)–C(11)	1.826(3)	P(5)–C(51)	1.823(3)
P(1)–C(22)	1.827(3)	P(5)–C(62)	1.827(3)
P(1)–C(28)	1.833(3)	P(5)–C(68)	1.831(3)
O(1)–C(21)	1.318(3)	O(5)–C(61)	1.323(3)
O(2)–C(21)	1.228(3)	O(6)–C(61)	1.228(3)
C(16)–C(21)	1.463(4)	C(56)–C(61)	1.458(4)
Cl(1)–Ru(1)–Cl(2)	89.24(2)	Cl(5)–Ru(5)–Cl(6)	89.99(2)
Cl(1)–Ru(1)–P(1)	87.44(2)	Cl(5)–Ru(5)–P(5)	87.81(2)
Cl(2)–Ru(1)–P(1)	85.96(2)	Cl(6)–Ru(5)–P(5)	85.25(2)
Cg1–Ru(1)–Cl(1)	124.07(4)	Cg6–Ru(5)–Cl(5)	122.76(4)
Cg1–Ru(1)–Cl(2)	126.27(4)	Cg6–Ru(5)–Cl(6)	126.16(4)
Cg1–Ru(1)–P(1)	130.63(4)	Cg6–Ru(5)–P(5)	131.78(5)
Cg2–Fe(1)–Cg3	179.11(6)	Cg7–Fe(5)–Cg8	179.15(6)
O(1)–C(21)–O(2)	123.1(2)	O(5)–C(61)–O(6)	122.8(2)
C(11)–P(1)–C(22)	101.2(1)	C(51)–P(5)–C(62)	101.4(1)
C(11)–P(1)–C(28)	104.8(1)	C(51)–P(5)–C(68)	105.0(1)
C(22)–P(1)–C(28)	103.9(1)	C(62)–P(5)–C(68)	103.3(1)
⟨Ar1, Cp1⟩	75.0(1)	⟨Ar5, Cp5⟩	76.5(1)
⟨Ar1, Ph1⟩	39.4(1)	⟨Ar5, Ph5⟩	40.2(1)
⟨Ar1, Ph2⟩	26.3(1)	⟨Ar5, Ph6⟩	29.3(1)
⟨Ph1, Ph2⟩	59.0(1)	⟨Ph5, Ph6⟩	59.7(1)
⟨Cp1, Cp2⟩	1.4(2)	⟨Cp5, Cp6⟩	1.3(2)

Atom in both molecules are numbered analogously; atom labels in molecule 2 are obtained by adding four to the first digit in the respective atom label in molecule 1. Definitions, ring plane: plane atoms (centroid): molecule A, Ar1: C(34–39) (Cg1), Cp1: C(11–15) (Cg2), Cp2: C(16–20) (Cg3), Ph1: C(22–27) (Cg4), Ph2: C(28–33) (Cg5); molecule B, Ar5: C(74–79) (Cg6), Cp5: C(51–55) (Cg7), Cp6: C(56–60) (Cg8), Ph5: C(62–67) (Cg9), Ph6: C(68–73) (Cg10).

in KBr; cf. 1666 cm<sup>-1</sup> for Hd<sub>2</sub>p in Nujol [11]) and significantly higher than the values observed for the related carboxylate salts (Nadp<sup>-</sup>: 1540 [11]; M(dpf)<sub>2</sub>, where M = Ca, Sr and Ba: 1535–1547 cm<sup>-1</sup> [16]) and carboxylate complex [(η<sup>5</sup>-C<sub>5</sub>HMe<sub>4</sub>)<sub>2</sub>Ti(dpf-κ<sup>2</sup>O,O')] (1506 cm<sup>-1</sup> [17]). IR spectrum of **5** in the same region (1300–1800 cm<sup>-1</sup>) showed weak

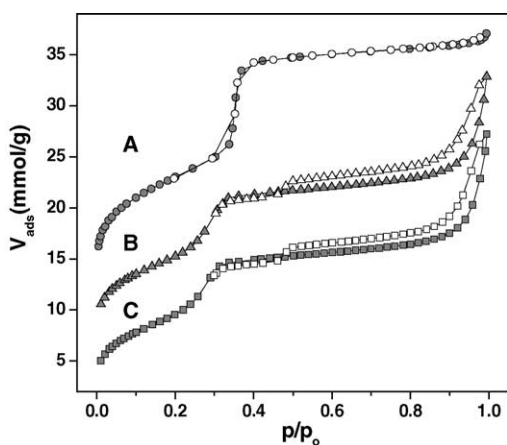


Fig. 3. Nitrogen adsorption isotherms of parent MCM-41 (A), **3** (B), and **4** (C). For clarity, isotherms B and C are onset by 5 and 10 mmol g<sup>-1</sup>, respectively.

Table 2  
Hydrogen bond parameters for 2-CH<sub>2</sub>Cl<sub>2</sub> (in Å and °)

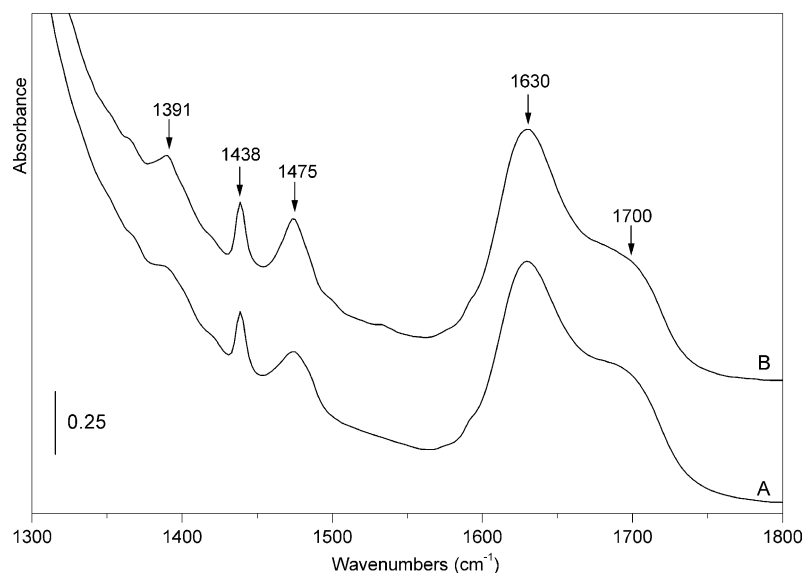
D–H···A	D–H	D···A	D–H···A
O(1)–H(1)···O(6) and (x – 1, y – 1, z)	0.82(4)	2.654(3)	177(5)
O(5)–H(5)···O(2) and (1 + x, 1 + y, z)	0.83(4)	2.654(3)	178(4)
C(91)–H(91A)···O(2)	0.97	3.175(4)	148
C(92)–H(92B)···O(6)	0.97	3.158(4)	145
C(91)–H(91B)···Cl(2)	0.97	3.657(3)	153
C(92)–H(92A)···Cl(6)	0.97	3.707(3)	153

Values involving hydrogen atoms in calculated positions are given without standard uncertainties. Labelling of the solvating dichloromethane: C(91)H(91A)H(91B)Cl(91)Cl(92) and C(92)H(92A)H(92B)Cl(93)Cl(94). D = donor, A = acceptor.

to medium-intensity bands (see Section 4) attributable to the organometallic modifier. The region of ν<sub>OH</sub> vibrations in IR spectra of all compound is dominated by a very broad band at ca. 3750 cm<sup>-1</sup>.

Table 3  
Textural properties of parent MCM-41 and the modified sieves **3** and **4**

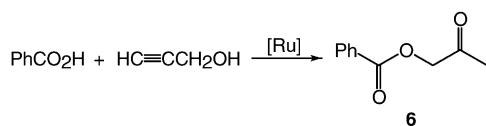
Sample (m <sup>2</sup> g <sup>-1</sup> )	S <sub>BET</sub> (cm <sup>3</sup> g <sup>-1</sup> )	V <sub>meso</sub> (nm)	d (nm)
MCM-41	1085	0.914	3.5
<b>3</b>	843	0.590	3.2
<b>4</b>	795	0.541	3.0

Fig. 4. IR spectra of **3** (A) and **4** (B).

In  $^{31}\text{P}$  CP MAS NMR spectra, the phosphorus containing sieves **3** and **4** showed resonances with quite similar chemical shifts,  $\delta_{\text{P}}$  33 and 35, respectively, which are both markedly down-field compared to the signal of uncoordinated Hd $\text{P}$  in  $\text{CDCl}_3$  solution ( $\delta_{\text{P}}$   $-17.6$  [11]), closer to values typical for  $P$ -coordinated Hd $\text{P}$  or the corresponding phosphine oxide (Hd $\text{P}$ o;  $\delta_{\text{P}}$  32.9 in  $\text{CDCl}_3$  [11]).

#### 2.4. Catalytic experiments

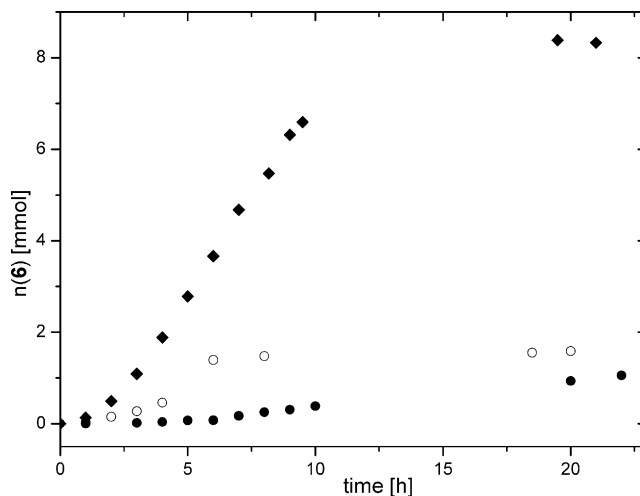
The testing reaction between benzoic acid and propargyl alcohol to give 2-oxopropyl benzoate (**6**) (Scheme 2) was performed in toluene with 0.5 mol% ruthenium precursor added either as a defined molecular compound (**2**) or in the supported form (**4** and **5**). In all cases, the reaction proceeded with the formation of the expected product **6**, however it was much faster with the molecular catalyst (Fig. 5). With the molecular catalyst **2** and 1.5-fold molar excess of propargyl alcohol with respect to the acid, about 84% of the acid was converted to **6** within 24 h at  $80^\circ\text{C}$  (Fig. 6) while the supported catalysts **4** and **5** under otherwise identical conditions produced **6** in yields lower than 20% (Fig. 7; 19% yield of **6** has been achieved with catalyst **4** after 68 h). In all cases, the ester starts to form after an induction period, which is significantly longer for the supported catalysts (see Figs. 5–7). This points to a necessary activation of the catalyst (formation of an catalytically active



Scheme 2.

species), which can also account for the catalyst leaching (see below).

Although one can expect the immobilized catalysts to exhibit an activity lower than the analogous homogeneous system, the low efficiency observed for the precatalysts **4** and **5** results also from the inherent properties of the sieve: MCM-41 behaves as a non-innocent support, promoting a parallel process, which is faster than the formation of **6** and converts propargyl alcohol to an unidentified, probably polymeric side product. This can be demonstrated by a much steeper decrease in the propargyl alcohol content in the reaction mixture containing catalyst **4** when compared to catalyst **2** (see Figs. 5–7). This side reaction occurs in a similar

Fig. 5. A comparison of the rate of ester **6** formation with catalyst **2** ( $\blacklozenge$ ), heterogenised catalyst **4** ( $\bullet$ ), and phosphine-free heterogenised catalyst **5** ( $\circ$ ).

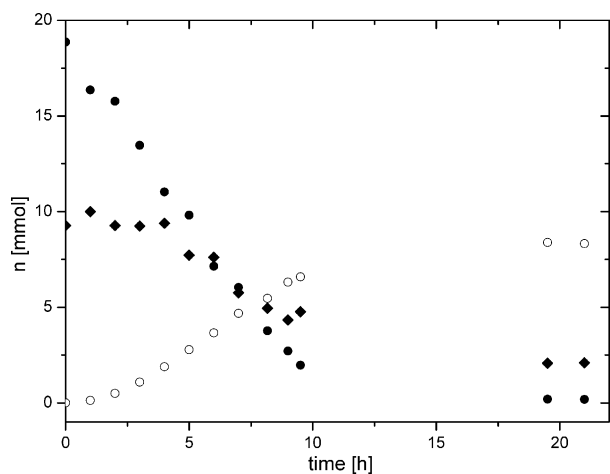


Fig. 6. Kinetic profile for the testing reaction with homogenous catalyst **2** (●, propargyl alcohol; ◆, benzoic acid; ○, ester **6**).

extent also when a solution of the alcohol is heated only with MCM-41 in toluene without addition of benzoic acid and a ruthenium compound. Attempts to improve the selectivity of the reaction by lowering the reaction temperature failed, the yields of **6** being even lower (ca. 0.4% at 40 °C and ca. 3.7% at 60 °C with the same educt ratio after 68 h).

When the immobilized catalysts **4** and **5** were removed after heating of the reaction mixture for 4 h (by centrifugation and filtration of the supernatant through a 0.45 μm PTFE syringe filter), the reaction did not stop but slowed down significantly (Fig. 8). This indicates some leaching of the active form of the catalyst during the reaction. Notably, when the catalyst was recovered from the cold reaction mixture after the experiment, washed well with toluene and reused at the same ratio (i.e., 5 mol% as calculated from the original Ru content), it showed activity as high as the original sample of the immobilized catalyst. The preserved catalyst activity can be accounted for a re-adsorption of active

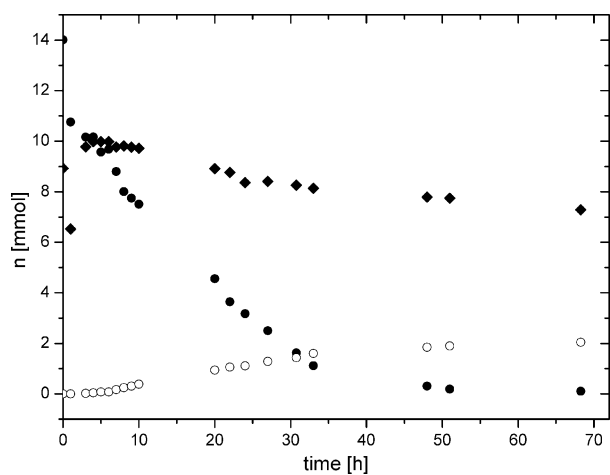


Fig. 7. Kinetic profile for the testing reaction with heterogenised catalyst **4** (●, propargyl alcohol; ◆, benzoic acid; ○, ester **6**).

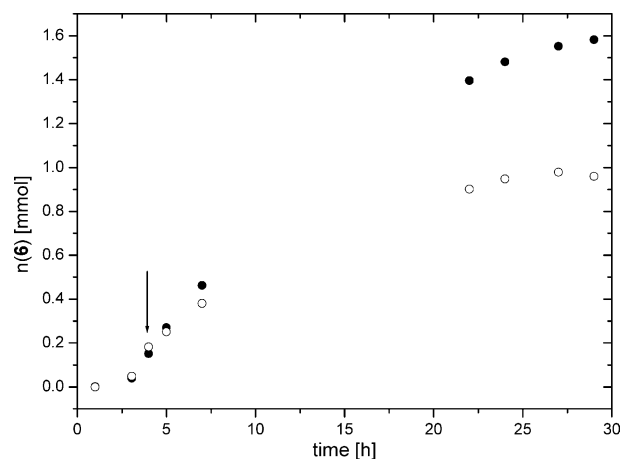


Fig. 8. A comparison of product formation in the mixture containing heterogenised catalyst **5** (●) and in the same system where the solid catalyst was removed after heating for 4 h (○, the removal time is indicated by an arrow).

ruthenium species after cooling the reaction mixture to room temperature.

### 3. Conclusions

The reaction of MCM-41 with Hdpf and **1** in a stepwise manner produced **4** while the direct treatment of the sieve with **1** gave Ru-only modified MCM-41, **5**. The spectral data did not allow us to draw clear conclusion about the nature of the interaction of the sieve with modifiers but indicated for **3** and **4** that Hdpf and **1** are anchored independently rather than in a form analogous to the molecular compound **2**. Considering the results of textural measurements (i.e., stepwise lowering of the surface area, the void volume and a decrease of the pore diameter) may indicate a simple sorption of the modifying agents in the pores and on the surface. This process is probably accompanied by an irreversible change at the phosphino moiety of Hdpf, which prevents it to ligate ruthenium.

In the reaction between propargyl alcohol and benzoic acid to give 2-oxopropyl benzoate, the supported materials are less active and selective than homogeneous precatalyst **2**, producing yet unknown, probably polymeric side product from propargyl alcohol, the latter property being inherent to the support (MCM-41). However, the presented results indicate that the metal-modifiers remain tightly bound to the support and, although some leaching occurs during catalyzed reaction, the supported materials can be reused at least once without a loss of their original activity. In addition, it is apparent that the preparation of supported catalyst may eliminate the need for the presence of stabilizing ligands, such as phosphines (see Ref. [12]). Despite the bonding between the modifiers and the solid support remains not fully understood, the early attempt at anchoring of Hdpf and **1** opens new possibilities in the immobilization of ferrocene ligands.

## 4. Experimental

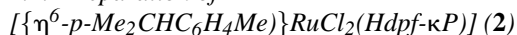
### 4.1. Materials and methods

All-siliceous MCM-41 was synthesized from sodium silicate (Riedel de Haen), hexadecyltrimethylammonium bromide (Fluka) and ethyl acetate (Fluka) at 100 °C for 50 h as described in detail in Refs. [18,19]. The template was removed by calcination in a stream of air at 550 °C for 6 h. Prior to the modification reactions, the sieve was dried at 200 °C Torr for 2 h.

Hdpf was prepared according to the literature procedure [11]. Complex **1** (Strem) was used without further purification. Dichloromethane was dried over potassium carbonate while toluene was dried over potassium metal and distilled under nitrogen. Syntheses of complex **2** and the supported compounds **3–5** were performed under argon blanket and the subsequent workup was carried out in air.

Solution  $^1\text{H}$  (399.95 MHz),  $^{31}\text{P}\{^1\text{H}\}$  (161.90 MHz), and  $^{13}\text{C}\{^1\text{H}\}$  NMR (100.58 MHz) spectra were measured at 25 °C on a Varian UNITY Inova 400 spectrometer. Chemical shifts ( $\delta$ , ppm) are given relative to internal tetramethylsilane ( $^1\text{H}$  and  $^{13}\text{C}$ ) and external 85% aqueous  $\text{H}_3\text{PO}_4$  ( $^{31}\text{P}$ ).  $^{31}\text{P}\{^1\text{H}\}$  solid-state NMR spectra were measured on a Varian spectrometer (121.473 MHz) at room temperature using the CP/MAS technique (5 mm rotor, spinning 5–7 kHz, contact time 1.5 ms) and solid  $(\text{NH}_4)_2\text{HPO}_4$  as the reference ( $\delta_{\text{P}} 0$ ). Positive-ion liquid secondary-ion mass spectra (LSIMS) were obtained on a VG ZabSpec spectrometer in 3-nitrobenzylalcohol matrix using CsI as the primary ion source ( $\text{Cs}^+$ ) and poly(ethylene glycol) as the mass scale calibrant for high-resolution (HR) measurements. IR spectra in KBr pellets were recorded on an FT IR Nicolet Protégé 460 spectrometer. X-ray powder diffractograms were recorded using a Siemens D5005 instrument operating in the Bragg-Brentano geometry arrangement using Cu K $\alpha$  radiation ( $\lambda = 1.5412 \text{ \AA}$ ). Nitrogen adsorption isotherms were measured at  $-196 \text{ }^\circ\text{C}$  on an ASAP 2010 (Micromeritics) equipped with a 133 kPa transducer. All samples were evacuated before measurement at 150 °C for at least 24 h. X-ray fluorescence analysis was carried out with a Philips PW 1404 using Uniquant analytical.

### 4.2. Preparation of



Solid **1** (0.459 g, 0.75 mmol) and Hdpf (0.621 g, 1.50 mmol) were dissolved in dichloromethane (30 mL). After stirring for 2 h, the solution was evaporated to dryness and the solid washed well with diethyl ether ( $2 \times 20 \text{ mL}$ ) and dried under vacuum (0.2 Torr/50 °C/1 h) to afford **2** as a rusty orange solid (1.052 g, 97%).  $^1\text{H}$  NMR ( $\text{CDCl}_3$ ):  $\delta$  0.93 (d,  $^3J_{\text{HH}} = 6.9 \text{ Hz}$ , 6H,  $\text{CHMe}_2$ ), 1.80 (s, 3H,  $\text{Me}$ ), 2.52 (septet,  $^3J_{\text{HH}} = 6.9 \text{ Hz}$ , 1H,  $\text{CHMe}_2$ ), 3.91 (apparent t, 2H, CH of  $\text{C}_5\text{H}_4\text{CO}_2\text{H}$ ), 4.40 (m, 4H, CH of  $\text{C}_5\text{H}_4\text{PPh}_2$  and  $\text{C}_5\text{H}_4\text{CO}_2\text{H}$ ), 4.63 (apparent q, 2H, CH of  $\text{C}_5\text{H}_4\text{PPh}_2$ ), 5.14

(d,  $J = 6.1 \text{ Hz}$ , 2H) and 5.19 (d,  $J = 5.7 \text{ Hz}$ , 2H) (AA'BB' system of  $\text{C}_6\text{H}_4$ ), 7.42–7.50 (m, 6H,  $\text{PPh}_2$ ), 7.83–7.90 (m, 4H,  $\text{PPh}_2$ ).  $^{13}\text{C}$  NMR ( $\text{CDCl}_3$ ):  $\delta$  17.1 (s,  $\text{Me}$ ), 21.7 (s,  $\text{CHMe}_2$ ), 30.0 (s,  $\text{CHMe}_2$ ), 70.2 (s,  $\text{C}_{\text{ipso}}$  of  $\text{C}_5\text{H}_4\text{CO}_2\text{H}$ ), 71.6 (s, CH of  $\text{C}_5\text{H}_4\text{CO}_2\text{H}$ ), 73.0 (d,  $J_{\text{PC}} = 8 \text{ Hz}$ , CH of  $\text{C}_5\text{H}_4\text{PPh}_2$ ), 75.6 (s, CH of  $\text{C}_5\text{H}_4\text{CO}_2\text{H}$ ), 76.6 (d,  $J_{\text{PC}} = 10 \text{ Hz}$ , CH of  $\text{C}_5\text{H}_4\text{PPh}_2$ ), 78.4 (d,  $^1J_{\text{PC}} = 48 \text{ Hz}$ ,  $\text{C}_{\text{ipso}}$  of  $\text{C}_5\text{H}_4\text{PPh}_2$ ), 86.0 (d,  $^2J_{\text{PC}} = 6 \text{ Hz}$ , CH of  $\text{C}_6\text{H}_4$ ), 90.3 (d,  $^2J_{\text{PC}} = 4 \text{ Hz}$ , CH of  $\text{C}_6\text{H}_4$ ), 94.5, 109.5 ( $2 \times \text{s}$ ,  $\text{C}_{\text{ipso}}$  of  $\text{C}_6\text{H}_4$ ); 127.8 (d,  $J_{\text{PC}} = 10 \text{ Hz}$ , CH of  $\text{PPh}_2$ ), 130.4 (d,  $J_{\text{PC}} = 2 \text{ Hz}$ , CH of  $\text{PPh}_2$ ), 133.9 (d,  $J_{\text{PC}} = 10 \text{ Hz}$ , CH of  $\text{PPh}_2$ ), 136.3 (d,  $^1J_{\text{PC}} = 47 \text{ Hz}$ ,  $\text{C}_{\text{ipso}}$  of  $\text{PPh}_2$ ), 177.0 (s,  $\text{CO}_2\text{H}$ ).  $^{31}\text{P}$  NMR ( $\text{CDCl}_3$ ):  $\delta$  19.3 (s). IR (KBr,  $\text{cm}^{-1}$ ):  $\nu_{\text{CH}}$  3054 (w), 2870 (w);  $\nu_{\text{C=O}}$  1702 (s), 1674 (s); 1471 (s), 1434 (s), 1386 (m), 1290 (m), 1159 (m), 1096 (m), 1029 (s); 835 (m), 746 (s), 698 (s); 540–469 (s, composite). Anal. calcd. for  $\text{C}_{33}\text{H}_{33}\text{Cl}_2\text{FeO}_2\text{PRu}$ : C, 55.02; H, 4.62%. Found: C, 55.41; H, 4.79%. HR LSIMS:  $[\text{C}_{33}\text{H}_{33}^{35}\text{Cl}_2^{56}\text{FeO}_2\text{P}^{102}\text{Ru}]^+$  ( $\text{M}^+$ ), calcd. 719.9994, found 719.9992;  $[\text{C}_{33}\text{H}_{33}^{35}\text{Cl}^{56}\text{FeO}_2\text{P}^{102}\text{Ru}]^+$  ( $[\text{M}-\text{Cl}]^+$ ), calcd. 685.0308, found 685.0300. LSIMS,  $m/z$  (relative intensity): 722 (2,  $\text{M}^+$ ), 685 (23,  $[\text{M}-\text{Cl}]^+$ ), 649 (82,  $[\text{M}-2\text{Cl}]^+$ ), 611 (11,  $[\text{M}-\text{C}_6\text{H}_5\text{O}_2]^+$ ), 485 (100,  $[\text{M}-\text{C}_6\text{H}_5\text{O}_2-2\text{Cl}]^+$ ), 414 (67,  $\text{Hdpf}^+$ ).

### 4.3. Preparation of MCM-41-supported Hdpf (**3**)

A solution of Hdpf (0.8285 g, 2.00 mmol) in toluene (200 ml) was added to MCM-41 (10.0 g). The mixture was shaken on a mechanical shaker for 24 h at room temperature. Then, the solid was separated by filtration, washed with toluene and dichloromethane and extracted with dichloromethane in a Soxhlet extractor for 8 h. A subsequent drying in air at ambient temperature afforded carboxyphosphine-modified MCM-41 (**3**) as a fine, brownish solid. Yield: 10.5 g.

The extract was evaporated under vacuum, leaving a rusty brown residue, which was analyzed as Hdpf by NMR spectroscopy (0.1354 g, 16% recovery). X-ray fluorescence analysis for **3**: P, 0.49; Fe, 0.87%. Calculated from mass balance (84% retention of Hdpf): P, 0.48; Fe, 0.87%. IR (KBr,  $\text{cm}^{-1}$ ): 1690, 1630, 1475, 1440, 1390, 752, 727, 704, 695.  $^{31}\text{P}$  CP-MAS NMR:  $\delta_{\text{P}}$  33.0.

### 4.4. Modification of the supported phosphine with **1**

Modified sieve **3** (8.00 g) was added to a solution of **1** (0.3833 g, 0.6259 mmol) in dichloromethane (65 ml). The mixture was stirred for 24 h at room temperature, the solid filtered off and washed well with dichloromethane and dried in air at room temperature to give Ru/P-modified MCM-41 (**4**). Yield: 8.0 g.

The solvent and washings were evaporated, leaving only 5.3 mg of a brown material, containing mostly unreacted **1** according to  $^1\text{H}$  NMR spectra. X-ray fluorescence analysis for **4**: P, 0.50; Fe, 0.92; Ru, 0.35%. Calculated from mass

balance assuming that 99% of **1** reacted: P, 0.48; Fe, 0.87; Ru, 1.54%. IR (KBr,  $\text{cm}^{-1}$ ): virtually identical to **3**.  $^{31}\text{P}$  CP-MAS NMR:  $\delta_{\text{P}}$  34.9.

#### 4.5. Preparation of Ru-modified MCM-41 (**5**)

A solution **1** (0.065 g, 0.11 mmol) in dichloromethane (20 ml) was added to MCM-41 (1.568 g) and the mixture was stirred for 22 h at room temperature. The solid was filtered off, washed well with dichloromethane ( $4 \times 15$  ml), and dried under vacuum. This procedure afforded Ru-modified molecular sieve **5** quantitatively and, as revealed by the analysis of the washing, with quantitative retention of Ru on the support (ca. 0.13 mmol Ru/g of the solid).

X-ray fluorescence analysis for **5**: Ru 0.09%. Calculated from mass balance (complete retention of **1** assumed): Ru 0.13%. IR (KBr,  $\text{cm}^{-1}$ ): 1745 (w), 1637 (m), 1461 (w), 1401 (w), 1384 (w). Powder X-ray diffraction:  $2\theta$  ( $^\circ$ ) 2.25 (s), 3.78 (m), 4.45 (m) and 5.92 (vw).

#### 4.6. Catalytic experiments

Catalytic experiments were carried out in a three-necked flask (50 ml) immersed in a thermostated oil bath ( $\pm 2^\circ$ ) and equipped with a magnetic stirring bar, thermometer, reflux condenser and a rubber septum. All experiments were performed under nitrogen.

A reaction mixture consisting of propargyl alcohol (0.89 ml, 0.15 mmol), benzoic acid (0.122 g, 10 mmol), mesitylene (internal standard; 0.28 ml, 2.0 mmol) and dry toluene (10 ml) was thoroughly mixed at preset reaction temperature. Then, the amount of a catalyst corresponding to 0.05 mmol (0.5 mol%) ruthenium was added. Reaction samples were periodically withdrawn by a syringe for at least 48 h (24 h for homogeneous catalyst **2**) and analyzed by a high-resolution gas chromatography (Agilent 6850 equipped with flame ionization detector and DB-5 capillary column). All reaction products were checked by GC-MS (Hewlett-Packard 5890 Series II, 5971A). A sample of pure ester **7** was obtained by chromatography of the reaction mixture (silica gel, hexane-ether). Analytical data for **6**: NMR ( $\text{CDCl}_3$ ):  $\delta_{\text{H}}$  2.24 (s, 3H, Me), 4.88 (s, 2H,  $\text{CH}_2$ ), 7.43–8.13 (m, 5H, Ph);  $\delta_{\text{C}}$  26.23 (Me), 68.75 ( $\text{CH}_2$ ), 128.52 (CH of Ph), 129.20 ( $\text{C}_{\text{ipso}}$  of Ph), 129.91 (CH of Ph), 133.48 (CH of Ph), 165.87 (COO), 201.83 (C(O)Me); MS:  $m/z$  (relative abundance) 178 ( $\text{M}^+$ , 8), 163 ( $[\text{M}-\text{CH}_3]^+$ , 10), 148 ( $[\text{M}-\text{CH}_2\text{CO}]^+$ , 20), 135 ( $[\text{M}-\text{CH}_2\text{COCH}_3]^+$ , 15), 122 ( $[\text{PhCO}_2\text{H}]^+$ , 2), 105 ( $[\text{PhCO}]^+$ , 100), 91 ( $[\text{C}_7\text{H}_7]^+$ , 5) 77 ( $\text{Ph}^+$ , 60), 51 ( $[\text{C}_4\text{H}_3]^+$ , 35); HR MS:  $\text{C}_{10}\text{H}_{10}\text{O}_3$  ( $\text{M}^+$ ), calcd. 178.0630, found 178.0641.

#### 4.7. X-ray crystallography

Recrystallization of **2** from dichloromethane-hexane afforded red, plate-like single-crystals of solvatomorph **2**· $\text{CH}_2\text{Cl}_2$ . The selected specimen (0.20 mm  $\times$

Table 4

Crystallographic data, data collection and structure refinement for **2**· $\text{CH}_2\text{Cl}_2$

Formula	$\text{C}_{34}\text{H}_{35}\text{Cl}_4\text{FeO}_2\text{PRu}$
$M$ ( $\text{g mol}^{-1}$ )	805.31
Crystal system	Triclinic
Space group	$P-1$ (no. 2)
$a$ ( $\text{Å}$ )	12.3808(2)
$b$ ( $\text{Å}$ )	12.7439(2)
$c$ ( $\text{Å}$ )	20.8371(3)
$\alpha$ ( $^\circ$ )	91.3979(9)
$\beta$ ( $^\circ$ )	95.508(1)
$\gamma$ ( $^\circ$ )	96.542(1)
$V$ ( $\text{Å}^3$ )	3249.11(9)
$Z$	4
$F(000)$	1632
$D_c$ ( $\text{g cm}^{-3}$ )	1.646
$\mu$ (Mo $\text{K}\alpha$ ) ( $\text{mm}^{-1}$ )	1.321 <sup>a</sup>
Collected diffractions	58536
$2\theta_{\text{max}}$ ( $^\circ$ )	55.0
Unique/observed <sup>b</sup> diffractions	14695/10321
$R_{\text{int}}$ (%) <sup>c</sup>	5.42
Number of parameters	783
$R$ observed diffractions (%) <sup>d</sup>	3.65
$R$ , $wR$ all data (%) <sup>d</sup>	6.44, 8.72
$\Delta\rho$ ( $\text{e Å}^{-3}$ )	1.30, $-0.87^e$

<sup>a</sup> Corrected for absorption (Gaussian correction based on the crystal shape), transmission coefficient range: 0.584–0.922.

<sup>b</sup> Diffractions with  $I_0 > 2(I_0)$ .

$$^c R_{\text{int}} = \frac{\sum |F_0^2 - \langle F_0^2 \rangle|}{\sum |F_0^2|}$$

$$^d R = \frac{\sum \|F_0\| - |F_c|}{\sum |F_0|}, wR = \left\{ \frac{\sum w(F_0^2 - F_c^2)^2}{\sum w(F_0^2)^2} \right\}^{1/2}$$

<sup>e</sup> See Section 3.7 for the discussion of the high residual electron density.

0.63 mm  $\times$  0.63 mm) was mounted on a glass fibre by epoxy cement and transferred to diffractometer. Full-set diffraction data ( $\pm h \pm k \pm l$ ) were collected on a Nonius KappaCCD diffractometer equipped with Cryostream Cooler (Oxford Cryosystems) at 150(2) K using graphite monochromatized Mo  $\text{K}\alpha$  radiation ( $\lambda = 0.71073 \text{ Å}$ ) and analyzed with HKL program package by Nonius BV (Table 4).

Cell parameters were determined by least-squares analysis from 40,700 partial diffractions with  $1.0 \leq \theta \leq 27.5^\circ$ . The structure was solved by direct methods (SIR97 [20]) and refined by weighted full-matrix least-squares procedure on  $F^2$  (SHELXL97 [21]). All non-hydrogen atoms were refined with anisotropic thermal motion parameters. The hydrogen atoms were included in calculated positions [C–H bond lengths: 0.96 Å (methyl), 0.97 Å (methylene), 0.98 Å (methine), and 0.93 Å (aromatic)] and assigned 1.5  $U_{\text{eq}}(\text{C})$  (methyl) and 1.2  $U_{\text{eq}}(\text{C})$  (all other). Isopropyl substituents at the Ru-coordinated arene ring exhibit a disorder, most likely due to an unhindered rotation along the pivotal C–C bond and, hence, the space occupied by these substituents accommodate the largest residual electron density. Attempted refinement of the isopropyl group over two or more positions failed. Final geometric calculations were performed with a recent version of Platon program [22].

Crystallographic data excluding the structure factors have been deposited with the Cambridge Crystallographic Data Centre [deposition no. CCDC-231990]. Copies of the data can be obtained upon request to CCDC, 12 Union Road, Cambridge CB21EZ, UK; <http://www.ccdc.cam.ac.uk>, e-mail: [deposit@ccdc.cam.ac.uk](mailto:deposit@ccdc.cam.ac.uk).

## Acknowledgements

The authors thank Dr. Ivana Císařová for collecting X-ray diffraction data, Dr. Arnošt Zúkal for recording nitrogen adsorption isotherms and Ing. Marcela Tkadlecová for recording solid-state NMR spectra. This work was supported by the Grant Agency of the Czech Republic (grant nos. 104/02/0571 and 203/99/M037) and is a part of a long-term Research Plan of the Faculty of Sciences, Charles University.

## References

- [1] (a) A. Togni, T. Hayashi (Eds.), *Ferrocenes*, VCH, Weinheim, 1995; (b) C.J. Richards, A.J. Locke, *Tetrahedron: Asymmetry* 9 (1998) 2377; (c) T.J. Colacot, *Chem. Rev.* 103 (2003) 3101.
- [2] (a) B. Gotov, Š. Toma, D.J. Macquarrie, *Enantiomer* 4 (1999) 263; (b) B. Gotov, Š. Toma, D.J. Macquarrie, *New J. Chem.* 24 (2000) 597; (c) R. Frantz, J.O. Durand, G.F. Lanneau, J.C. Jumas, J. Olivier-Fourcade, M. Persin, *Eur. J. Inorg. Chem.* (2002) 1088, For use of phosphonic groups in immobilization of ferrocene compounds, see:.
- [3] C.T. Kresge, M.E. Leonowicz, W.J. Roth, J.S. Beck, *Nature* 359 (1992) 710.
- [4] F. Schüth, *Chem. Mater.* 13 (2001) 3184.
- [5] J. Čejka, *Appl. Catal. A* 54 (2003) 327.
- [6] J.Y. Ying, Ch.P. Mehnert, M.S. Wong, *Angew. Chem. Int. Ed.* 38 (1999) 56.
- [7] D.E. De Vos, I.F.J. Vankelekom, P.A. Jacobs (Eds.), *Chiral Catalyst Immobilization and Recycling*, Wiley–VCH, Weinheim, 2000.
- [8] A. Severeys, D.E. De Vos, L. Fiermans, F. Verpoort, P.J. Grobet, P.A. Jacobs, *Angew. Chem. Int. Ed.* 40 (2001) 586.
- [9] H. Balcar, J. Sedláček, J. Čejka, J. Vohlídal, *Macromol. Rapid Commun.* 23 (2002) 32.
- [10] (a) B.F.G. Johnson, S.A. Raynor, D.S. Shepherd, T. Mashmeyer, J.M. Thomas, G. Sankar, S. Bromley, R. Oldroyd, L. Gladden, L. Mantle, *Chem. Commun.* (1999) 1167; (b) S.A. Raynor, J.M. Thomas, R. Raja, B.F.G. Johnson, R.G. Bell, M.D. Mantle, *Chem. Commun.* (2000) 1925; (c) T.J. Colacot, *Chem. Rev.* 103 (2003) 3101.
- [11] J. Podlaha, P. Štěpnička, I. Císařová, J. Ludvík, *Organometallics* 15 (1996) 543.
- [12] (a) D. Devanne, C. Ruppín, P.H. Dixneuf, *J. Org. Chem.* 53 (1988) 926; (b) C. Bruneau, Z. Kabouche, M. Neveux, B. Seiller, P.H. Dixneuf, *Inorg. Chim. Acta* 222 (1994) 155; (c) C. Bruneau, P.H. Dixneuf, *Chem. Commun.* (1997) 507 (a review).
- [13] P. Štěpnička, R. Gyepes, O. Lavastre, P.H. Dixneuf, *Organometallics* 16 (1997) 5089.
- [14] J.F. Mai, Y. Yamamoto, *J. Organomet. Chem.* 560 (1998) 223.
- [15] (a) P. Štěpnička, R. Gyepes, J. Podlaha, *Collect. Czech. Chem. Commun.* 63 (1998) 64; (b) P. Štěpnička, J. Podlaha, R. Gyepes, M. Polášek, *Organomet. J. Chem.* 552 (1998) 293; (c) P. Štěpnička, I. Císařová, J. Podlaha, J. Ludvík, M. Nejezchleba, *Organomet. J. Chem.* 582 (1999) 319; (d) L. Lukešová, J. Ludvík, I. Císařová, P. Štěpnička, *Collect. Czech. Chem. Commun.* 65 (2000) 1897.
- [16] P. Štěpnička, J. Podlaha, *Inorg. Chem. Commun.* 1 (1998) 332.
- [17] K. Mach, J. Kubišta, I. Císařová, P. Štěpnička, *Acta Crystallogr. C* 58 (2002) m116.
- [18] J. Čejka, A. Krejčí, N. Žilková, J. Dědeček, J. Hanika, *Microporous Mesoporous Mater.* 44–45 (2001) 499.
- [19] G. Schulz-Ekloff, J. Rathouský, A. Zúkal, *J. Porous. Mater.* 1 (1999) 97.
- [20] A. Altomare, M.C. Burla, M. Camalli, G.L. Casciarano, C. Giacovazzo, A. Guagliardi, G.G. Moliterni, G. Polidori, R. Spagna, *J. Appl. Cryst.* 32 (1999) 115.
- [21] G.M. Sheldrick, SHELXL97, Program for Crystal Structure Refinement from Diffraction Data, University of Göttingen, Göttingen, 1997.
- [22] A.L. Spek, Platon, a multipurpose crystallographic tool, 2001. Available via the Internet at <http://www.cryst.chem.uu.nl/platon>.